Ultrathin composite polymeric membranes for CO_2/N_2 separation with minimum thickness and high CO_2 permeance

Javier Benito[1], Javier Sánchez-Laínez[2], Beatriz Zornoza[2], Santiago Martín[3], Mariolino Carta[4], Richard Malpass-Evans[4], Carlos Téllez[2], Neil B. McKeown[4], Joaquín Coronas[2]* and Ignacio Gascón[1]*

[1]Instituto de Nanociencia de Aragón (INA) and Departamento de Química Física, Universidad de Zaragoza, C/ Pedro Cerbuna 12, 50009 Zaragoza (Spain).
[2]Instituto de Nanociencia de Aragón (INA) and Departamento de Ingeniería Química y Tecnologías del Medio Ambiente, Universidad de Zaragoza, C/ Mariano Esquillor, s/n., 50018 Zaragoza (Spain).
[3]Instituto de Ciencia de Materiales de Aragón (ICMA) and Departamento de Química Física, CSIC-Universidad de Zaragoza, C/ Pedro Cerbuna 12, 50009 Zaragoza (Spain).
[4]School of Chemistry, University of Edinburgh, David Brewster Road, Edinburgh, EH9 3FJ (UK).

* E-mail: coronas@unizar.es (Prof. Dr. J. C.); igascon@unizar.es (Dr. I. G.)

Keywords: Composite membranes • Gas separation • Monolayers • Polymers • Post-combustion

Abstract: The use of ultrathin films as selective layers in composite membranes offers significant advantages in gas separation for increasing productivity whilst reducing the membrane size and energy costs. In this contribution, composite membranes have been obtained by the successive deposition of ca. 1 nm thick monolayers of a polymer of intrinsic microporosity (PIM) on top of dense membranes of the ultra-permeable poly[1-(trimethylsilyl)-1-propyne] (PTMSP). The ultrathin PIM films (30 nm in thickness) demonstrate CO_2 permeance up to 7 times higher than dense PIM membranes using only 0.04% of the mass of PIM without a significant decrease in CO_2/N_2 selectivity.

Polymeric membranes offer advantages in gas separation processes compared to other technologies like cryogenic distillation or selective adsorption in terms of energy efficiency.[1] An ideal membrane should be as thin as possible, to maximize the flux (i.e. permeance) across the membrane, as selective as possible, to achieve an efficient separation, and mechanically robust.[2] Thus, the development of ultrathin (i.e. less than 100 nm) membranes without losing selectivity is an attractive target.[3] For composite multi-layer membranes, the cost of the polymer selective layer would be significantly reduced using ultrathin films, therefore allowing the use of high-cost, high-performance materials. This is of particular importance for large-scale gas separations such as carbon capture membrane where the required surface area of the membrane will be many square km.[4]

Polymers of intrinsic microporosity[5],[6] (PIMs) are a class of polymers with excellent performance for gas separations demonstrating both high permeability (e.g. PCO_2 > 1000 Barrer) and moderate selectivity (e.g. PCO_2/PN_2 ~ 20). Highly rigid PIMs composed of bridged bicyclic units such as ethanoanthracene (EA) and Troger Base (TB)[7] are of particular interest due to their higher selectivity.

In order to obtain ultrathin layers of PIM, we considered the Langmuir-Blodgett (LB) technique[8] which can be used for the deposition of polymeric layers on top of different kinds of supports to produce composite membranes. Using this approach, LB films formed by different surfactants have been previously deposited onto poly[1-(trimethylsilyl)-1-propyne] (PTMSP) as substrates in order to enhance selectivities for H_2/CO_2[9] and CO_2/N_2[10] separations. Ultrapermeable PTMSP films have been also used as support for the deposition of metal-organic covalent networks by chemical vapor deposition for gas separation membranes.[11] Because of its extraordinarily high gas permeability, [12] PTMSP is commonly used as gutter layer in composite membranes.[13] Moreover, solvent cast PTMSP films present an almost flat surface and, consequently, they are very suitable supports for the deposition of polymer ultrathin selective films.

Here, we report the successive deposition of monolayers of a polymer of intrinsic microporosity, PIM-EA-TB(H_2), on top of PTMSP membranes using the Langmuir-Schaefer (LS) horizontal deposition method[14] (see Scheme 1).

The use of the LB method to prepare ultrathin films for gas separation usually requires sophisticated strategies to obtain selective films[3] (photo cross-linking, hydrogen bonding, ionic cross-linking). In this contribution, we have shown that PIM-EA-TB(H_2) forms homogeneous and stable monolayers at the air-water interface (see supporting

information and Figure S1) that can be transferred onto different substrates using the LS method.

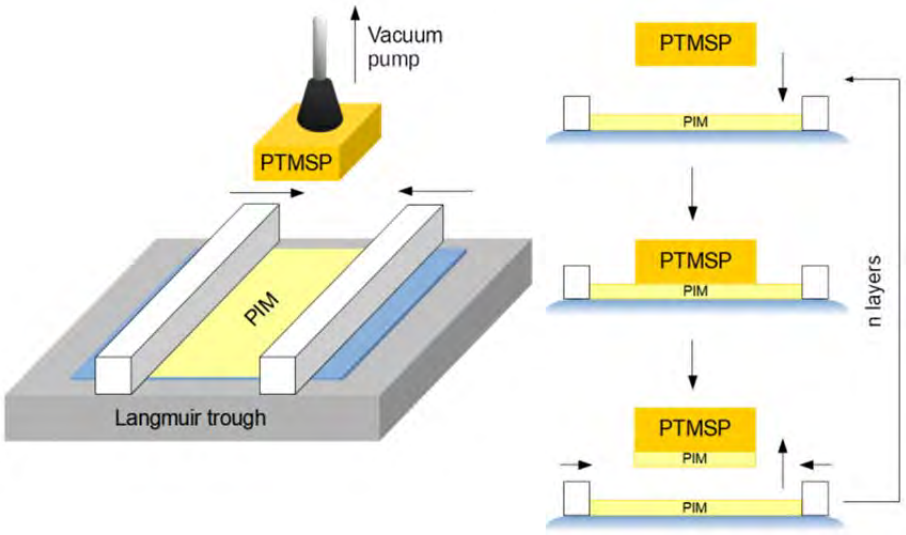

Scheme 1. Langmuir-Schaefer horizontal deposition of PIM-EA-TB(H_2) monolayers onto PTMSP membrane. One monolayer is deposited each time that the membrane contacts the film floating on the water surface.

Each PIM-EA-TB(H_2) LS monolayer deposited had a thickness of ca. 1 nm and several monolayers could be successively deposited using this procedure to obtain an ultrathin selective layer with the desired thickness. The total number of PIM-EA-TB(H_2) monolayers deposited depends on the number of times (*n*) that the substrate contacts during the down stroke the PIM film floating on the water surface.

LS films deposited onto different solid substrates have been characterized using UV-vis and X-ray photoelectron spectroscopy (XPS), thermogravimetric analysis (TGA) and atomic force microscopy (AFM). Further details about film fabrication and characterization can be found in the supporting information and Figures S2 to S7.

LS films deposited onto quartz substrates show an almost constant increase of the film absorbance with the number of layers up to n = 30 (Figure 1) revealing a continuous and constant PIM-EA-TB(H_2) deposition between 1 and 30 monolayers.

Additionally, XPS spectra provided information about the elemental composition of the surface of PTSMP/PIM_n composite membranes, incorporating a known number (*n*) of PIM-EA-TB(H_2) monolayers (Table 1 and Figures S5 to S7).

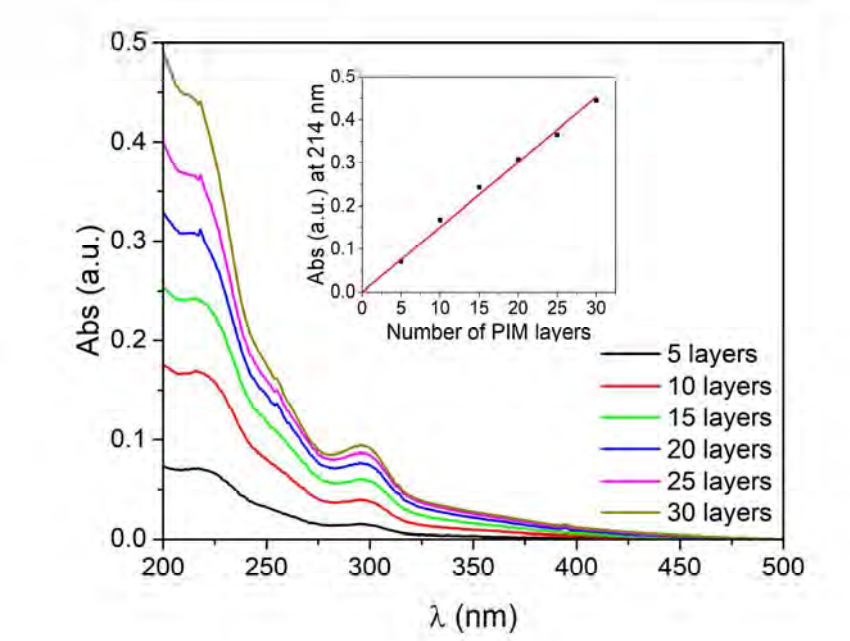

Figure 1. UV-vis spectra of PIM LS films deposited onto quartz (inset: Absorbance at λ = 214 nm vs. number of PIM-EA-TB(H_2) LS layers deposited).

In a bare PTMSP membrane, the nitrogen content was negligible, while the silicon content was 11.7%. For PTMSP/PIM_n membranes, when the number of LS PIM monolayers deposited increased from 1 to 10, the Si content gradually fell down to 1.6% at the same time that the N content increased up to 7.6% confirming the growth of the stacking of PIM-EA-TB(H_2) on top of the PTMSP membrane with each LS deposition.

Table 1. Surface atomic percentages of C, N and Si in polymeric membranes determined by XPS.

Membrane	% C	% N	% Si
bare PTMSP	88.3	-	11.7
PTMSP/PIM_1	87.9	3.5	8.6
PTMSP/PIM_5	90.3	6.7	3.0
PTMSP/PIM_10	90.8	7.6	1.6

AFM characterization was used to analyze the thickness and roughness of the membranes (Figure 2 and Figure S3). Bare PTMSP membranes present a root mean square roughness (RMS) of 1.06 nm. When one LS PIM-EA-TB(H_2) film was

deposited, the RMS of the PTMSP/PIM_1 membrane (0.88 nm) was similar or even lower than in the pure PTMSP membrane. This confirms that the deposition of the PIM-EA-TB(H_2) monolayer did not significantly modify the textural roughness of the PTMSP membrane, allowing the deposition of successive polymer layers. Additionally, a ca. 1 nm thickness of the LS monolayer was determined measuring the height profile in different film borders (Figure 2b).

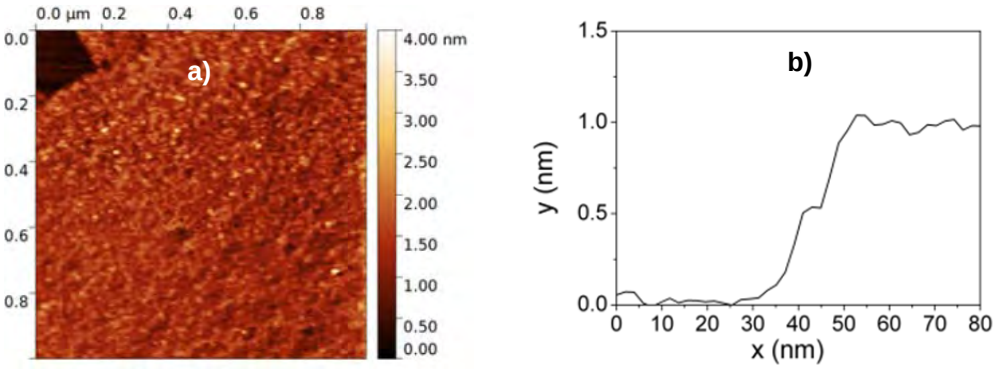

Figure 2. a) AFM characterization of PTMSP/PIM_1 composite membrane (only 1 LS PIM monolayer deposited). The thickness of the PIM-EA-TB(H_2) LS film was obtained measuring the height in different film borders as shown in b).

The density of PIM LS films has been estimated considering the molar mass of the monomer (270 g·mol^{-1}), the area per monomer at the surface pressure of transference (0.31 nm^2·monomer^{-1}) and the height of the monolayer (1 nm). The value obtained (1.45 g·cm^{-3}) is significantly higher than the experimental density reported for structurally similar polymer PIM-EA-TB (1.08 g·cm^{-3})[15] which reveals that this methodology allows the deposition of compact PIM monolayers.

PTSMP/PIM_n composite membranes, incorporating between 1 to 30 PIM monolayers, have been tested for CO_2/N_2 separation in post-combustion conditions (35 ºC, feed pressure 1-3 bar, CO_2/N_2 mixture composition in volume 10/90). These membranes demonstrate a gradual increase of selectivity with *n* (Figure 3 and Table S1). The goal of this study was to determine the minimum number of PIM-EA-TB(H_2) layers required to achieve similar selectivity to that obtained from dense thick films of the same selective polymer.

As shown in Figure 3a, dense PTMSP membranes (thickness ca. 80 µm) showed high CO_2 permeance (371 GPU) but low CO_2/N_2 selectivity (4.4). Dense PIM-EA-TB(H_2) membranes (thickness also ca. 80 µm) showed a much lower CO_2 permeance (18 GPU)

but improved CO_2/N_2 selectivity (15.4), while PTSMP/PIM_30 membranes (thickness of selective layer = 30 nm) presented a CO_2/N_2 selectivity of 13.5 close to that of the pure PIM-EA-TB(H_2) membrane but with a significantly higher CO_2 permeance of 114 GPU. Consequently, this methodology resulted in membranes of CO_2 permeance almost 7 times larger than that of the dense PIM-EA-TB(H_2) membrane.

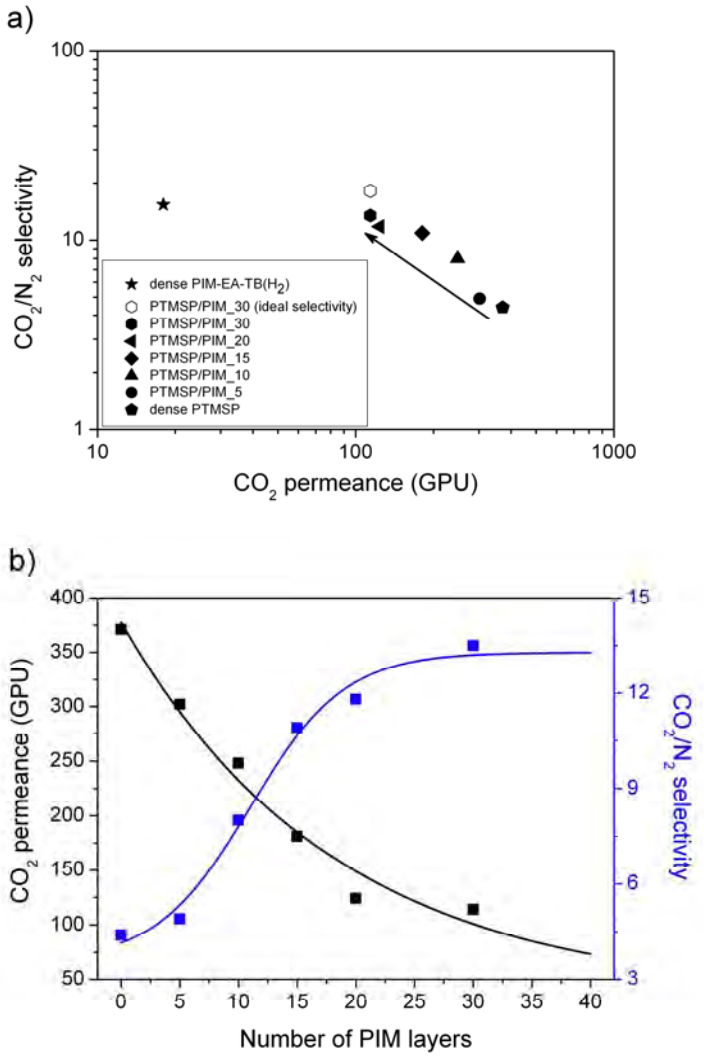

Figure 3. CO_2/N_2 separation performance of polymeric membranes studied in post-combustion conditions (CO_2/N_2 mixture composition, in volume, 10/90; 35 ºC and feed pressure 3 bar). a) comparison of thick dense membranes of bare polymers and composite membranes formed by 5-30 monolayers of PIM-EA-TB(H_2) deposited onto dense PTMSP. The arrow indicates the tendency when the number of LS PIM-EA-TB(H_2) films deposited increases. b) Separation performance of polymeric membranes vs. number of PIM-EA-TB(H_2) monolayers deposited onto PTMSP. Symbols are experimental data and solid lines fitted curves using simple equations (exponential decay for CO_2 permeance and Boltzmann sigmoid function for CO_2/N_2 selectivity).

Moreover, single gas permeation was also studied for the PTSMP/PIM_30 membrane. For proper comparison with previously published results, the CO_2/N_2 ideal selectivity (the ratio of single gas permeances) was also calculated, reaching a value of 18.2. This value is in good agreement with the best results published for dense membranes of the structurally similar polymer PIM-EA-TB[15] (CO_2/N_2 selectivity values reported depend on the activation procedure and measuring device and oscillate between 13 and 19).

For membranes with a number of PIM-EA-TB(H_2) monolayers below 20, an increase in the feed pressure (Table S1 and Figure S8) caused a decrease in the CO_2/N_2 selectivity that may be related to defects in the ultrathin PIM layers. With a higher numbers of layers the selectivity remained almost constant at feed pressures between 1 and 3 bar, suggesting the achievement of an almost defect-free ultrathin selective layer, in agreement with the overall increase in the selectivity. Furthermore, a basic mathematical fitting of the composite membrane performance with the number of PIM monolayers allowed determining that 30 PIM monolayers optimize the selectivity and CO_2 permeance of composite membranes (see Figure 3b).

A simple comparison between the mass of PIM used for the fabrication of the ultrathin selective layer (thickness = 30 nm) in PTSMP/PIM_30 composite membranes and the amount of PIM mass in dense membranes (thickness = 80 µm) allows obtaining that the PIM content in composite membranes is only 0.04% of the PIM dense membrane.

To gain insight into the microscopic membrane structure, a cross-section of a PTMSP/PIM_30 (30 layers) sample was characterized by SEM (Figure 4a). It is possible to distinguish a coating of about 30 nm that corresponds to the stacking of 30 PIM-EA-TB(H_2) LS monolayers with a different contrast to that of the lower PTMSP dense membrane.

The elemental composition of two sections of PTMSP/PIM_30 was analyzed by focused ion beam-scanning electron microscopy (FIB-SEM). This allows cutting the membrane with nanometer resolution (up to 5 nm) by using sputtered Ga^+ ions in a selected area (10×5 µm in this specimen) obtaining a smooth surface. Energy-dispersive X-ray spectroscopy (EDX) was used to obtain a mapping of this sample, (Figure 4b) showing that N (green) coming from PIM-EA-TB(H_2) polymer was mainly in the upper part of the membrane while Si (red) corresponding to PTMSP was found in the bottom part.

Furthermore, a lamella of the membrane was cut for analysis by transmission electron microscopy (TEM). The sequence of images of the lamella thinning can be found in the

supporting information (Figure S9). A TEM image of the lamella is depicted in Figure 4c which confirms the thickness of about 30 nm for the PIM-EA-TB(H_2) multilayer film (30 LS).

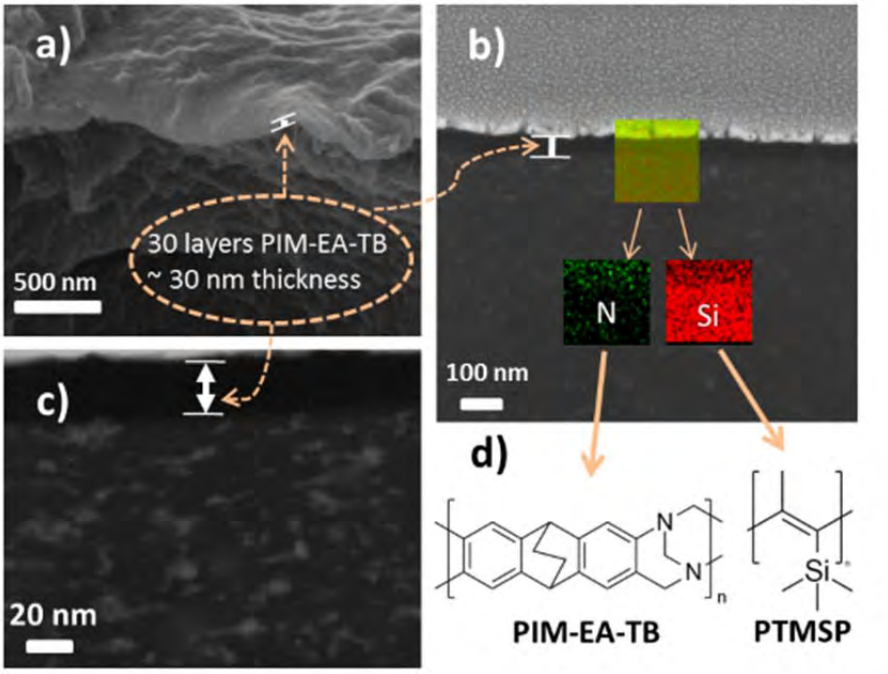

Figure 4. Electron microscopy images of the composite membrane PTMSP/PIM_30 with a thickness (measured in 15 different points along the sample) of 30.5±5.2 nm of PIM-EA-TB(H_2) layer (30 LS films deposited onto PTMSP): a) SEM cross-section, b) focused ion beam with an inset including an EDX mapping (N in green and Si in red), c) TEM image from a lamella extracted from the sample specimen and d) chemical structure of the polymers forming the composite membrane.

It should be highlighted that all the membranes prepared in this contribution were manipulated exactly in the same manner and no differences were observed between the mechanical properties of composite and dense membranes. Moreover, a preliminary study of the stability of a composite PTMSP/PIM_30 membrane was performed and promising results were obtained. 5 weeks after the first gas separation study (at 35 ºC and 3 bar) CO_2 permeance was reduced from 109 to 94 GPU and CO_2/N_2 selectivity was increased from 13.5 to 14.5. This behavior improves significantly the reported performance for PTMSP that suffers physical aging (a reduction of 80% CO_2 permeance has been observed for a PTMSP membrane coated on a polyacrylonitrile

support during an operation period of 14 days[13]). The long-testing stability of the composite membranes will be the subject of further analysis in the future.

In conclusion, we have shown that using the LS method it is possible to deposit a controlled number of monolayers of a polymer of intrinsic microporosity, PIM-EA-TB(H_2), on top of PTMSP dense membranes to produce effective composite membranes for CO_2/N_2 post-combustion separation. Membranes with a selective PIM-EA-TB(H_2) layer only 30 nm thick (i.e. 0.04% of the PIM dense membrane content) present CO_2/N_2 selectivity similar to that of the dense PIM-EA-TB(H_2) with a CO_2 permeance 7 times larger.

In future works, this study will be extended to the deposition of other polymers of interest for gas separation in order to probe that this methodology can be used for different materials and processes.

Experimental Section

PIM-EA-TB(H_2) was synthesized as reported for PIM-EA-TB[7] from 2,6(7)-diaminoanthracene by reaction with dimethoxymethane in trifluoroacetic acid. Monolayer films of PIM-EA-TB(H_2) were fabricated at the air-water interface using a commercial KSV-NIMA trough and transferred at constant surface pressure (= 30 $mN \cdot m^{-1}$) onto solid substrates (quartz, mica and PTMSP dense membranes) for characterization and CO_2/N_2 separation studies. Gas separation studies were performed by feeding a 10/90 (in volume) CO_2/N_2 mixture at 35 °C and three different feed pressures (1, 2 and 3 bar). More details about experimental procedures and results can be found in the supporting information.

Acknowledgements

The research leading to these results has received funding from the EU PF7 Programme (FP7/2007-2013), under grant agreement number 608490, project M4CO2, Spanish MINECO and FEDER (MAT2016-77290-R) and the Aragon Government (T05 and E54). J. S.-L. thanks the Spanish Education Ministry Program FPU2014 for a Ph.D. grant. The microscopy work was carried out in the Laboratorio de Microscopías Avanzadas at the Instituto de Nanociencia de Aragón (LMA-INA, Universidad de Zaragoza).

References

[1] P. Bernardo, E. Drioli, G. Golemme, *Ind. Eng. Chem. Res.* **2009**, *48*, 4638-4663.

[2] Z. Zheng, R. Grünker, X. Feng, *Adv. Mater.* **2016**, *28*, 6529-6545.

[3] M. H. Wang, V. Janout, S. L. Regen, *Acc. Chem. Res.* **2013**, *46*, 2743-2754.

[4] B. Seoane, J. Coronas, I. Gascon, M. E. Benavides, O. Karvan, J. Caro, F. Kapteijn, J. Gascon, *Chem. Soc. Rev.* **2015**, *44*, 2421-2454.

[5] N. B. McKeown, P. M. Budd, *Chem. Soc. Rev.* **2006**, *35*, 675-683.

[6] N. B. McKeown, P. M. Budd, *Macromolecules* **2010**, *43*, 5163-5176.

[7] M. Carta, R. Malpass-Evans, M. Croad, Y. Rogan, J. C. Jansen, P. Bernardo, F. Bazzarelli, N. B. McKeown, *Science* **2013**, *339*, 303-307.

[8] K. Ariga, Y. Yamauchi, T. Mori, J. P. Hill, *Adv. Mater.* **2013**, *25*, 6477-6512.

[9] M. H. Wang, S. Yi, V. Janout, S. L. Regen, *Chem. Mater.* **2013**, *25*, 3785-3787.

[10] C. Lin, Q. B. Chen, S. Yi, M. H. Wang, S. L. Regen, *Langmuir* **2014**, *30*, 687-691.

[11] N. D. Boscher, M. H. Wang, A. Perrotta, K. Heinze, M. Creatore, K. K. Gleason, *Adv. Mater.* **2016**, *28*, 7479-7485.

[12] T. Masuda, E. Isobe, T. Higashimura, K. Takada, *J. Am. Chem. Soc.* **1983**, *105*, 7473-7474.

[13] Z. Dai, L. Ansaloni, L. Deng, *Green Energy & Environment* **2016**, *1*, 102-128.

[14] J. Y. Park, R. C. Advincula, *Soft Matter* **2011**, *7*, 9829-9843.

[15] E. Tocci, L. De Lorenzo, P. Bernardo, G. Clarizia, F. Bazzarelli, N. B. McKeown, M. Carta, R. Malpass-Evans, K. Friess, K. Pilnacek, M. Lanc, Y. P. Yampolskii, L. Strarannikova, V. Shantarovich, M. Mauri, J. C. Jansen, *Macromolecules* **2014**, *47*, 7900-7916.